

Estimation of tree height using UAV photogrammetric data

Rotimi-Williams Bello^{1*}, Pius A. Owolawi², E. A. van Wyk³, C. Tu⁴

^{1,2,3,4}Department of Computer Systems Engineering, Faculty of Information and Communication Technology, Tshwane University of Technology, South Africa; sirbrw@yahoo.com (R.W.B.), owolawipa@tut.ac.za (P.A.O.), vanwykea@tut.ac.za (E.A.W.), duc@tut.ac.za (C.T.).

Abstract: Dimensional characterization of trees plays important roles in phytoremediation project of precision agriculture and environmental protection. The dimensional characterization can be evaluated by using UAV-based geomatic surveys. The work in this study applies low-cost UAV photogrammetry for tree height estimation, particularly for a phytoremediation project on contaminated soils. Two locations that had differing mean tree heights (7m and 4m) were used for the purpose of study. Three different UAV flights were carried out at 40m, 50m, and 60m altitudes in Area 1, an olive grove, and two different flights at 45m and 52m altitudes in Area 2, which has poplar species. The Structure from Motion (SfM) method, Vegetation Filter (VF), Digital Surface Models (DSMs), and Raster computational tool were used to process the UAV point clouds in order to produce Canopy Height Models (CHMs) for a local maximum driven extraction of tree height. Relatively, the results obtained from the tree height estimation experiment for the locations using UAV are higher than the results obtained using in-field measurement, thereby justifying the suitability of UAV photogrammetric data for tree height estimation.

Keywords: Environmental protection, Photogrammetry, SfM, Tree height, UAV.

1. Introduction

Modern agricultural practice involves using high performing scientific, technological and analytical tools such as sensors to improve agricultural produce and assist management decisions. Precision agriculture as one of those strategic practices, in order to determine the appropriate inputs for maximum agricultural yield, addresses specific crop and livestock management through analysis and consideration of a number of factors [1]. Data collection from different sources and sensors such as geomatics is a crucial step in precision agriculture approach for obtaining better understanding of plant characterization and crop monitoring [2]. Precision agriculture comprises divers state-of-the-art techniques, that if combined, can improve the management of agriculture for its utmost sustainability [3].

However, there is a need for proper management of the data collected which can be handled by basic techniques such as geophysics and geomatics of geographic information systems (GISs) for precision agriculture management [4]. Geophysical survey involves the systematic method of collecting geophysical data of plants and soil for spatial studies. Geophysical methods measure the physical properties of materials that can be used to deduce information regarding the surface and subsurface of the earth using georadar systems, and their like [5]. Geomatics comprises the tools use in collecting, integrating and managing geospatial (geographic) data such as allowing empirical morphological description of the plants.

The application of UAV in precision agriculture was as a result of the challenges faced in using any of the satellite constellations solely for agricultural solutions on a local, regional or global basis [6]. Drone application in precision agriculture became more pronounced over two decades ago for its

affordability and compatibility with tools such as LiDAR (Light Detection And Ranging), multi-spectral, and optical cameras. Datasets and imagery acquired by LiDAR and multi-spectra are majorly used by researchers to analyse agricultural benefits of UAV acquired data [7-10]. This method is necessary for tree crown identification and classification particularly when the applications are constructed and applied in forest environment full of tall and dense trees [11-17].

Recently, in addition to LiDAR, photogrammetry datasets have been employed to carry out studies over lower vegetation areas [18-25], and several researchers have addressed the extraction of the height of tree with different characteristics using imagery acquired by UAV [26-30]. The results obtained from using photogrammetric data are not accurate as the ones obtained using LiDAR point clouds; this is due to insufficient information provided by photogrammetric data on the entire topography [31]. On the contrary, with LiDAR data, there is provision for easy access to information about the ground level by mere manipulation of return echoes (in their number) passing through the canopy [32]. The representation of the ground using this procedure, though by using expensive tools and compatible platforms, produces more accurate results for a vegetation 3D modelling [33].

Agricultural data as example of spatial data are analysed using any of the raster methods based on individual models such as canopy height models (CHMs), digital surface models (DSMs) or the hybrid of raster data and point clouds [34]. The crowns and heights of tree are important contributory factors for tree health estimation, and this is achieved by CHM application which is produced from operation carried out on the digital surface models (DSMs) and the like which can be produced by automatic filters exploitation for the identification of points symbolizing the surface of the ground. Initially, the purpose for designing vegetation filters (VF) was to handle LiDAR datasets; employing VF in photogrammetric applications has got wide acceptance [35].

Automatic filters are implemented by different software which have shown great performance in managing the thick forests vegetation better than the thin forests vegetation full of sparse trees [20-25], which are commonly used as agricultural fields for growing fruits and crops [36]. This trend continues with agricultural soils which have been contaminated by heavy-metals and pollutants; and the surest remedy is by applying phytoremediation approach [37]. Usually, agricultural scene images are structurally made in 2-dimension (2D) which need to be estimated in 3D structure; Structure from Motion (SfM) is a process that facilitates this estimation. However, SfM algorithm has some notable limitations that limit its capacity when it comes to extraction of low trees heights; this was addressed in [38].

The work reported in this paper is a part of work in progress and a step towards achieving tree height estimation by using UAV photogrammetric data, particularly for a phytoremediation project on contaminated soils. To achieve this aim, two locations that had differing mean tree heights (7m and 4m) were used for the purpose of study. Three different UAV flights were carried out at 40m, 50m, and 60m altitudes in Area 1, an olive grove, and two different flights at 45m and 52m altitudes in Area 2, which has poplar species. The Structure from Motion (SfM) method, Vegetation Filter (VF), Digital Surface Models (DSMs), and Raster computational tool were employed to process the UAV point clouds in order to produce Canopy Height Models (CHMs) for a local maximum driven extraction of tree height.

Relatively, the results obtained from the tree height estimation experiment for the two locations using UAV were compared to the results obtained when in-field measurement was employed.

2. Materials and Method

The main hardware materials employed for this study are UAV, UAV-captured photogrammetric data, and computer systems. For the software materials cum methods, we employed SfM, VF, DSMs and CHMs. Figure 1 shows the drone in Digital Image and Signal Processing (DISPLAY) Laboratory at Tshwane University of Technology (TUT), South Africa.



Figure 1.
Drone in digital image and signal processing (Display) lab at TUT.

2.1. Study Location

The study location comprises two areas, namely Area 1 and Area 2 that had differing tree characteristics, particularly in mean heights (7m and 4m). Area 1 has an olive grove; Area 2 has poplar species. Analysis of the experiment was carried out with the aim of determining whether the same height extraction technique could be used under various circumstances in order to assess any potential procedural constraints. As earlier mentioned, Area 1 which has its location on approximately 10,000 square meters land at Soshanguve of South Africa comprises mainly olive grove spread. At the time of carrying out this survey, mature olive trees of average height of 7m are predominant at the location.

An important reason for choosing the Area 1 location for our study is its possession of tree heights (7m on the average) including other favourable characteristics such as foliage density and canopy extension. Area 2, on the contrary comprises poplar species of mature trees (4m on the average) on 5,000 square meters land. Figure 2 shows the UAV-captured images of (a) Area 1, and (b) Area 2. The poplar tree is a deciduous tree that can grow up to 16m high and it suckers without restriction. The poplar tree is a problem at Mpumalanga Province of South Africa, and easily spread by wind-dispersed seeds that may travel long distances. Many indigenous riverine species have been replaced by the poplar tree. Moreover, the dense stands that formed as a result of suckering from the roots can become a barrier to free flow of water channels, thereby causing flooding and significant reduction in stream flow. The survey was carried out in March, 2024.

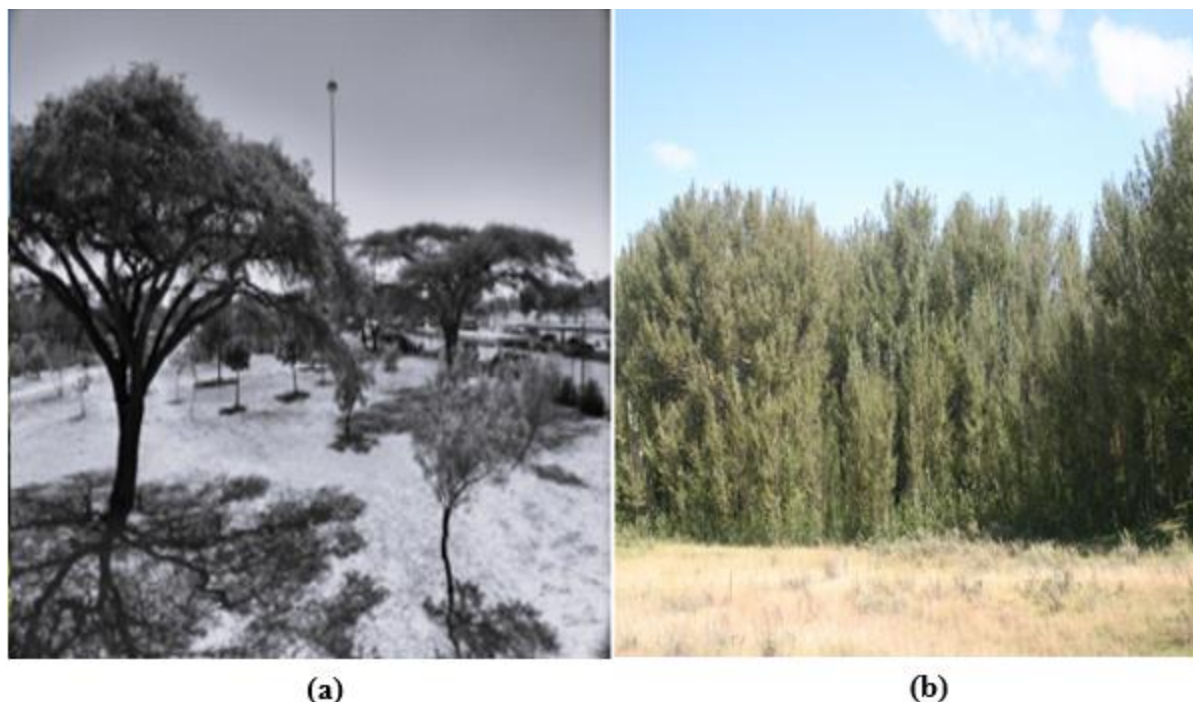


Figure 2.
UAV-captured images of (a) Area 1, and (b) Area 2.

2.2. Drone Specifications for Photogrammetry Survey

The DJI Mavic 3 Thermal is a state-of-the-art drone specifically designed for thermal imaging and inspection tasks, offering a suite of advanced features ideal for detailed analysis of photogrammetric captured images. The key specifications that underscore the capability of the flight conducted for the survey are presented in Table 1.

Table 1.
DJI Mavic 3 thermal specifications.

Thermal imaging camera	Visual imaging camera	Flight performance	Drone design	Additional features
1) Resolution: 640 × 512 pixels 2) Frame rate: 30 Hz 3) Field of view (FOV): 61° × 47° 4) Thermal sensitivity (NETD): ≤ 50 mK at f/1.0 5) Temperature measurement range: -20°C to 150°C, 0°C to 500°C (High gain mode)	1) Sensor: 1/2" CMOS, 12 MP 2) Video resolution: Up to 4K (3840 × 2160) at 30fps 3) Field of view (FOV): 56° horizontal 4) Digital zoom: Capable of up to 32× digital zoom for close inspection.	1) Maximum flight time: Approximately 45 minutes under optimal conditions. 2) Maximum speed: 72 km/h in sport mode. 3) Maximum transmission distance: 15 km, supported by the O3+ transmission system. 4) Obstacle	1) Weight: Approximately 920 grams. 2) Dimensions: 221 × 96.3 × 90.3 mm (folded), 347.5 × 283 × 107.7 mm (unfolded).	1) Satellite navigation: Supports GPS, GLONASS, and Galileo. 2) RTK compatibility: Optional integration with the D-RTK 2 Mobile Station for enhanced positioning accuracy. 3) Intelligent flight modes:

Thermal imaging camera	Visual imaging camera	Flight performance	Drone design	Additional features
6) Image processing enhancements: Features integrated advanced image processing technologies, including MSX for enhanced image detail.		detection: Provides omnidirectional sensing (Forward, backward, upward, downward, and lateral) for enhanced flight safety.		Includes smart tracking, waypoint flight, and AI spot-check for efficient and automated inspection processes.

The DJI Mavic 3 Thermal's high-resolution thermal and visual imaging capabilities, coupled with its advanced flight features, make it an excellent tool for precise and efficient capturing of photogrammetric images. Its modern design and portability further distinguish it from other thermal imaging solutions, such as the FLIR Vue Pro, by providing a comprehensive and versatile photogrammetric platform.

2.3. UAV Data Processing

On the same day under the same atmospheric conditions, three different UAV flights, namely F1, F2, and F3 were carried out at 40m, 50m, and 60m altitudes respectively in Area 1, an olive grove using the drone, DJI Mavic 3 Thermal with the specifications mentioned in Table 1. To guide against holes in our final generated output, the flights were manually conducted to ensure nothing less than the recommended overlapping of 60% Endlap and 40% Sidelap are obtained; with this precaution, we obtained 70% for Endlap and 60% for Sidelap. A Ground Control Points (GCPs), which is a land-based system was used to provide us the capability to observe, control and monitor the flights. Knowing that a good GCP distribution can help in image orientation, we evenly distributed 5 GCPs for central and edges coverage.

For Area 2 survey, we used the same UAVs used for Area 1 survey for the flights, namely F4 and F5, but on 45m and 52m altitudes respectively. To guide against holes in our final generated output, the flights were automatically conducted to ensure nothing less than the recommended overlapping of 60% Endlap and 40% Sidelap are obtained; with this precaution, we obtained 70% for Endlap and 60% for Sidelap. A Ground Control Points (GCPs), which is a land-based system was used to provide us the capability to observe, control and monitor the flights. Knowing that a good GCP distribution can help in image orientation, we evenly distributed 5 GCPs for central and edges coverage.

Agisoft Metashape was used to process the collected pictures. For the purpose of creating orthophotos, digital elevation models, and three-dimensional models, the geomatics community and geomatics expert frequently apply the commercial software package Metashape. The SfM method and Multiview Stereo (MVS) approaches are handled by Metashape. The MVS algorithms are capable of constructing 3D models with detailed information from images alone. The SfM technique makes it possible to reconstruct a limited representation of the scene and entirely orient the images automatically. Bundle block adjustment was used to optimize the camera calibration parameters, the spatial places of the tracks, and the position of the photos globally. Figure 3 shows the dense point cloud for filtering.



Figure 3.
Dense point cloud.

The UAV flights planning for UAV dataset capturing is shown in Figure 4. The workflow implementation in the software was adhere to. The workflow comprises sequential operations perform on the images, they are: (1) Import, (2) Alignment, (3) Sparse point cloud generation, (4) Alignment optimization, (5) Dense point cloud elaboration, and (6) Georeferencing. While flights F1, F2, and F3 acquired 81, 96, 105 nadiral frames respectively, flights F4 and F5 acquired 285 and 301 nadiral frames respectively with proper alignment. In Area 1, for each point cloud, the flights F1, F2, and F3 have approximately 77 million points (2.18 GB in size), 100 million points (2.44 GB in size), and 102 million points (2.46 GB in size) respectively. In Area 2, flights F4 and F5 have 110 million points (2.67 GB in size) and 115 million points (2.79 GB in size) respectively.

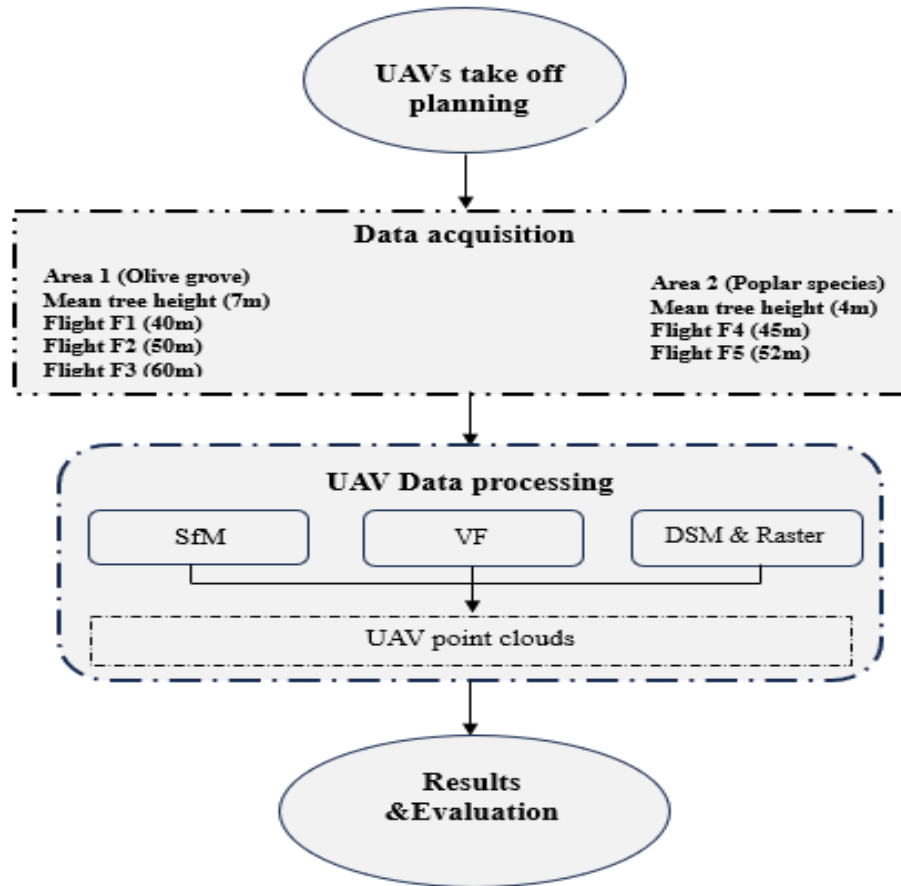


Figure 4.
The UAV flights planning for UAV dataset capturing and processing.

2.4. CHM-based Approach for Tree Height Extraction

The map representing the variation in height of individual trees at the two locations (Area 1 and Area 2) were computed using Equation (1) as follows:

$$CHM = DSM - DTM \quad (1) \quad [39]$$

where,

a DSM represents the surface of the earth including all objects on it. In contrast to a DSM, a DTM represents the surface of the earth (bare-ground surface) excluding all objects on it such as plants and buildings.

Local maxima approach was employed for the analysis of CHM maps in the GIS environment. Using the local maxima approach, the tree heights can be determined from among the pixel different values retrieved with the maximum value chosen as the tree heights candidacy which can be attributed to UAV as its derived tree heights. The values obtained for CHM was analysed using Zonal Statistic tool which makes it possible for the statistical computation of the raster's pixels in the regions. The next stage was extraction and matching of maximum values to individual trees for further operation. Figure 5 shows the extraction workflow of the tree heights.

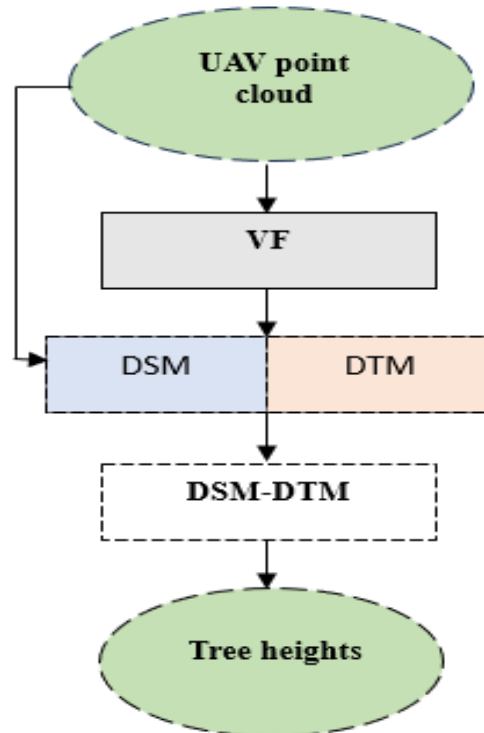


Figure 5.
The extraction workflow of the tree heights.

As shown in Figure 4, the validation of the tree heights extraction involves using the UAV-derived data and the in-field measurements. Therefore, by employing procedure of GIS, the positions of trees and values obtained from field measurements were matched, thereby obtaining comprehensive information about the area and the trees. Different statistical computations were made to evaluate the accuracy of the tree height experiment. Equation (2) shows the differences between each tree height extracted by UAV (denoted as $h_{\text{predicted},i}$) and the in-field measurements (denoted as $h_{\text{measurement},i}$) represented by Residuals (r).

$$r_i = h_{\text{predicted},i} - h_{\text{measurement},i} \quad (2)$$

Where,

$h_{\text{predicted}}$ is the UAV predicted height and $h_{\text{measurement}}$ is the measured height.

3. Results and Discussions

The interface for carrying out the photogrammetric surveys of tree heights estimation was designed and developed as shown in Figure 6. The interface allows different tree images to be selected and display for processing, the number of trees and their estimated heights are part of the interface design. The results obtained in Area 1 are not far from the results predicted for the employed method for tree heights estimation at locations with thick and tall trees justifying the chosen residual mean absolute values [40]. The flying altitudes of the three flights in Area 1 determined their performance, with flight F1 obtaining 80% of residuals less than 60cm. The performance of other two flights, flight F2 and flight F3 in terms of percentage of residuals was less than F1; this is evident in lower flying altitude achieving consistency relation of the trees.

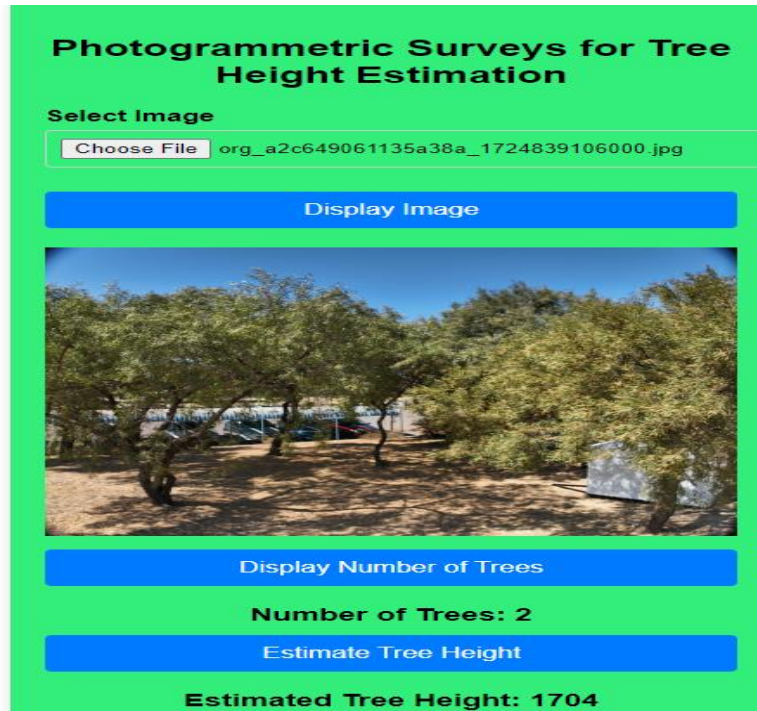


Figure 6.
The interface for performing photogrammetric surveys.

Differing results are likely to be obtained under different scenarios as observed in the results obtained by the three flights employed for Area 1 survey. Underestimation and overestimation of tree heights during flights planning are some of the reasons responsible for the differing results obtained from the survey. So, flight F2 and flight F3 obtained differing results because each flight either underestimated or overestimated the tree heights. In addition, the size of the location where flight F1 surveyed nearly influenced the normal distribution of the differences but for the number of trees, approximately, a normal distribution of the differences close to zero centre was observed. Figure 7 shows the graphical illustration of the tree count and height.

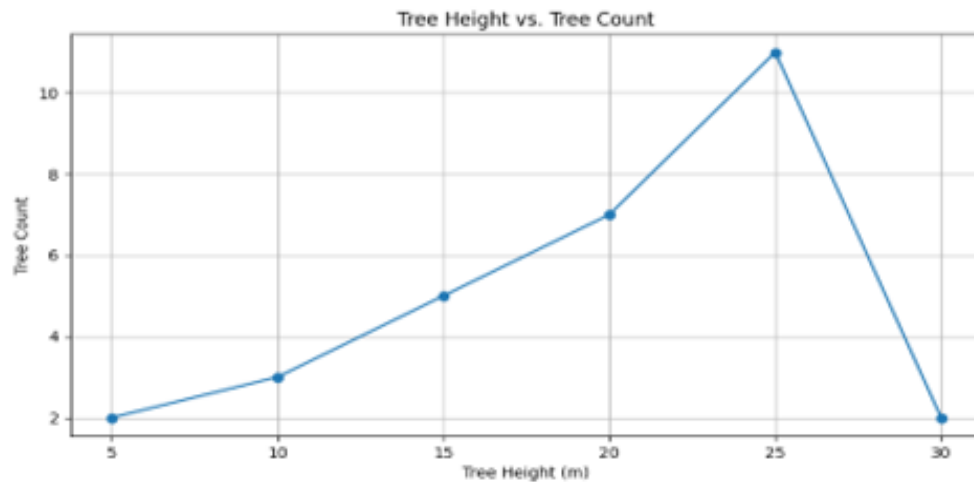


Figure 7.
Graphical illustration of the tree count and height.

Worthy of taking note are the continuous high interest and policy guiding agricultural lands in terms of use and management [41]. Many agricultural related fields are undergoing developmental transformation by the application of photogrammetric methods through geomatic surveys to provide agricultural solutions. The use of photogrammetric data for tree height estimation was the aim of the work carried out in this study. We present the results obtained from the UAV-captured imagery after statistical and computational analysis. Our methods employed photogrammetric procedure based on (SfM) method, Vegetation Filter (VF), Digital Surface Models (DSMs), and Raster computational tool. Figure 8 shows the residual differences between each tree height extracted by UAV and the in-field measurements in Area 1 for flights F1, F2, and F3 (label a), and in Area 2 for flights F4 and F5 (label b).

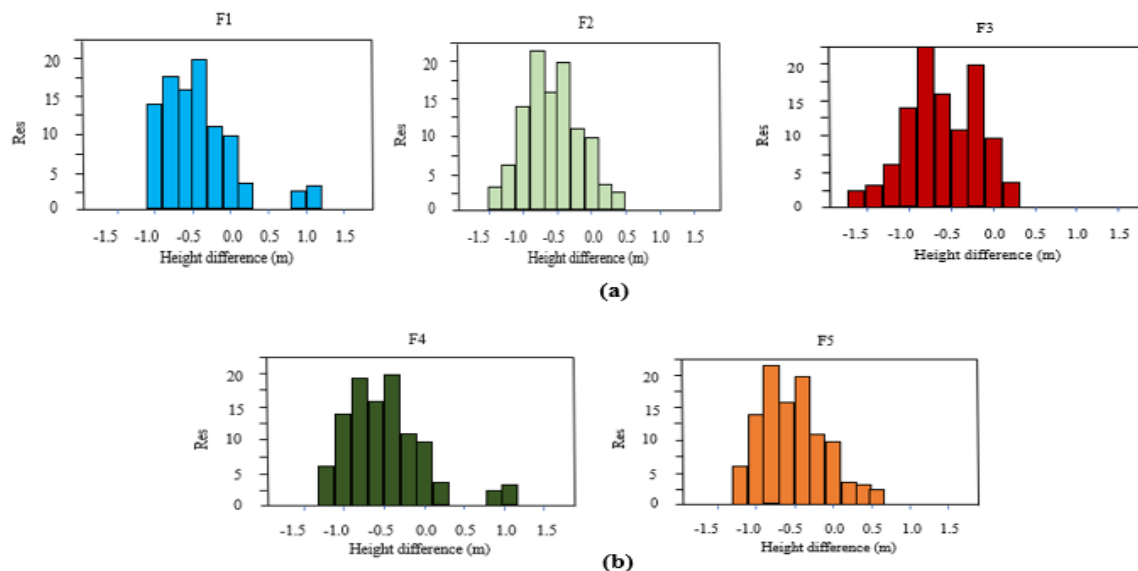


Figure 8.

Chart showing the residual differences between each tree height extracted by UAV and the in-field measurements in Area 1 for flights F1, F2, F3 (label a), and in Area 2 for flights F4 & F5 (Label b).

These models, either as an individual or combined, in addition to other open-source software employed for the surveys and analysis, made the procedural analysis in this study flexible and unambiguous. A total of five flights at different altitudes were carried out at the two study locations chosen for the assignment, namely Area 1, an olive grove, and Area 2, a poplar species. The application of filtering procedures to earth surface and vegetation enabled the generation of reference DTMs from the UAV dense point clouds. The CHMs representing the tree heights and obtained as represented in Equation (1) were analysed using the local maxima approach. Local maxima approach was employed for the analysis of CHM maps in the GIS environment so that the tree heights can be determined from among the pixel different values retrieved with the maximum value chosen as the tree heights candidacy which can be attributed to UAV as its derived tree heights.

The assessment of the proposed method accuracy was based on the in-field measurements and the UAV surveys which played significant role in the validation process and the computation. Among the existing related work that relatively supported our work findings are Pourreza et al. [42] who employed drone-based UAV flights at three differing altitudes at a location with tall trees; their findings established the axioms that flight altitudes influence accuracy. The flying altitudes of the three flights in Area 1 determined their performance, with Flight F1 obtaining 80% of residuals less than 60cm. The performance of other two flights, flight F2 and flight F3 in terms of percentage of residuals was less than F1; this is evident in lower flying altitude achieving consistency relation of the trees.

Underestimation and overestimation of tree heights during flights planning are some of the reasons responsible for the differing results obtained from the survey. So, flights F2 and F3 obtained differing results because each flight either underestimated or overestimated the tree heights. In so far as many other studies present findings that support the underestimation of tree heights during UAV flights as some of the reasons responsible for differing extracted heights [42], there is a need for further research, if not now, then definitely as a future work. The survey findings in Area 2 are different from the Area 1 in percentage residuals which has the mean tree heights as 4m. The individual tree heights have more influence on the accuracy of the tree heights estimation than the flight altitudes.

Accuracy in photogrammetric dense cloud representation of average tree heights, and influence of interpolation in generating and balancing DSM and DTM values are two main factors that affected the results reported in this study.

4. Conclusions

Estimation of tree height using UAV photogrammetric data has been presented in this paper. With the focus on precision agriculture and environmental protection; the study examines the usage of low-cost UAV photogrammetry for tree height estimation. The surveys involved two research locations that had different tree heights, namely Area 1 and Area 2. Using photogrammetric processing through the Structure from Motion (SfM) technique, Vegetation Filter (VF), Digital Surface Models (DSMs), and Raster computational tool, the UAV point clouds were processed to produce Canopy Height Models (CHMs) which was employed to compute the map representing the variation in height of individual trees at the two survey locations.

The results obtained in Area 1 are not far from the results predicted for the employed method for tree heights estimation at locations with thick and tall trees justifying the chosen residual mean absolute values. The flying altitudes of the three flights in Area 1 determined their performance, with flight F1 obtaining 80% of residuals less than 60cm. The performance of other two flights, flight F2 and flight F3 in terms of percentage of residuals was less than F1; this is evident in lower flying altitude achieving consistency relation of the trees.

The paper emphasizes the potential of UAVs for tree height measurement, particularly in situations with taller vegetation. For improved accuracy, future studies could make use of lower aircraft altitudes, cutting-edge technology like LiDAR, and the combination of oblique and nadiral photos.

Acknowledgement:

The authors received funding from the Tshwane University of Technology, South Africa.

Copyright:

© 2024 by the authors. This article is an open access article distributed under the terms and conditions of the Creative Commons Attribution (CC BY) license (<https://creativecommons.org/licenses/by/4.0/>).

References

- [1] E. F. I. Raj, M. Appadurai and K. Athiappan, "Precision farming in modern agriculture: In Smart agriculture automation using advanced technologies: Data analytics and machine learning, cloud architecture, automation and IoT," Singapore: Springer, 2022, pp. 61-87.
- [2] M. A. AbdelRahman, E. Farg, A. M. Saleh, M. Sayed, K. Abutaleb, S. M. Arafat, and M. M. Elsharkawy, "Mapping of soils and land-related environmental attributes in modern agriculture systems using geomatics," *Sustainable Water Resources Management*, vol. 8, no. 4, p. 116, 2022.
- [3] L. F. Oliveira, A. P. Moreira, and M. F. Silva, "Advances in agriculture robotics: A state-of-the-art review and challenges ahead," *Robotics*, vol. 10, no. 2, p. 52, 2021.
- [4] P. Ghosh and S. P. Kumpatla, "GIS applications in agriculture. In Geographic Information Systems and Applications in Coastal Studies," IntechOpen, 2022. <https://doi.org/10.5772/intechopen.104786>
- [5] F. Giannino and G. Leucci, "Electromagnetic methods in geophysics: applications in GeoRadar, FDEM, TDEM, and AEM," John Wiley & Sons, 2021

- [6] V. Martos, A. Ahmad, P. Cartujo and J. Ordoñez, “Ensuring agricultural sustainability through remote sensing in the era of agriculture 5.0,” *Applied Sciences*, vol. 11, no. 13, p. 5911, 2021.
- [7] C. L. Norton, K. Hartfield, C. D. H. Collins, W. J. van Leeuwen and L. J. Metz, “Multi-temporal LiDAR and hyperspectral data fusion for classification of semi-arid woody cover species,” *Remote Sensing*, vol. 14, no. 12, p/ 2896, 2022.
- [8] M. Semela, “Mapping and modelling above ground biomass in a mountainous terrain using multi-source remote sensing and environmental data,” Doctoral dissertation, University of the Free State, 2020.
- [9] Q. Hao, Y. Song, J. Cao, H. Liu, Q. Liu, J. Li, ... and L. Liu, “The development of snapshot multispectral imaging technology based on artificial compound eyes,” *Electronics*, vol. 12, no. 4, p. 812, 2023.
- [10] J. Liu, B. Yang, M. Li, and D. Xu, “Assessing forest-change-induced carbon storage dynamics by integrating GF-1 image and localized allometric growth equations in Jiangning District, Nanjing, Eastern China (2017–2020)” *Forests*, vol. 15, no. 3, p. 506, 2024.
- [11] S. Dersch, A. Schöttl, P. Krzystek and M. Heurich, “Semi-supervised multi-class tree crown delineation using aerial multispectral imagery and lidar data,” *ISPRS Journal of Photogrammetry and Remote Sensing*, vol. 216, pp. 154–167, 2024.
- [12] F. Naveed, B. Hu, J. Wang and G. B. Hall, “Individual tree crown delineation using multispectral LiDAR data,” *Sensors*, vol. 19, no. 24, p. 5421, 2019.
- [13] M. Dalponte, L. Frizzera and D. Gianelle, “Individual tree crown delineation and tree species classification with hyperspectral and LiDAR data,” *PeerJ*, vol. 6, p. e6227, 2019.
- [14] J. Marrs and W. Ni-Meister, “Machine learning techniques for tree species classification using co-registered LiDAR and hyperspectral data,” *Remote Sensing*, vol. 11, no. 7, p. 819, 2019.
- [15] K. Xu, Q. Tian, Y. Yang, J. Yue and S. Tang, “How up-scaling of remote-sensing images affects land-cover classification by comparison with multiscale satellite images” *International Journal of Remote Sensing*, vol. 40, no. 7, pp. 2784–2810, 2019.
- [16] S. Bramha, G. S. Bhunia, S. R. Kamlesh and P. K. Shit, “Comparative assessment of forest deterioration through remotely sensed indices—a case study in Korba District (Chhattisgarh, India),” In: *Spatial Modeling in Forest Resources Management. Environmental Science and Engineering*, Cham: Springer, pp. 153–173, 2021, https://doi.org/10.1007/978-3-030-56542-8_6
- [17] A. Ambadkar, P. Kathe, C. B. Pande and P. Diwate, “Assessment of spatial and temporal changes in strength of vegetation using normalized difference vegetation index (NDVI) and enhanced vegetation index (EVI): a case study from Akola District, Central India,” In *Geospatial Technology to Support Communities and Policy: Pathways to Resiliency*, Cham: Springer Nature Switzerland, pp. 289–304, 2024.
- [18] N. Anders, J. Valente, R. Masselink and S. Keesstra, “Comparing filtering techniques for removing vegetation from UAV-based photogrammetric point clouds,” *Drones*, vol. 3, no. 3, p. 61, 2019.
- [19] D. Pinton, A. Canestrelli, B. Wilkinson, P. Ifju and A. Ortega, “Estimating ground elevation and vegetation characteristics in coastal salt marshes using UAV-based LiDAR and digital aerial photogrammetry,” *Remote Sensing*, vol. 13, no. 22, p. 4506, 2021.
- [20] S. I. Jiménez-Jiménez, W. Ojeda-Bustamante, M. D. J. Marcial-Pablo and J. Enciso, “Digital terrain models generated with low-cost UAV photogrammetry: Methodology and accuracy,” *ISPRS International Journal of Geo-Information*, vol. 10, no. 5, p. 285, 2021.
- [21] F. Agüera-Vega, M. Agüera-Puntas, P. Martínez-Carricondo, F. Mancini and F. Carvajal, “Effects of point cloud density, interpolation method and grid size on derived digital terrain model accuracy at micro topography level,” *International Journal of Remote Sensing*, vol. 41, no. 21, pp. 8281–8299, 2020.
- [22] A. Šiljeg, M. Barada, I. Marić and V. Roland, “The effect of user-defined parameters on DTM accuracy—development of a hybrid model” *Applied geomatics*, vol. 11, pp. 81–96 2019.
- [23] D. Ali-Sisto, R. Gopalakrishnan, M. Kukkonen, P. Savolainen and P. Packalen, “A method for vertical adjustment of digital aerial photogrammetry data by using a high-quality digital terrain model” *International Journal of Applied Earth Observation and Geoinformation*, vol. 84, p. 101954, 2020.
- [24] M. Aleshin, L. Gavrilova A. Melnikov, “Use of unmanned aerial vehicles on example of Phantom 4 (standard) for creating digital terrain models,” *Engineering for Rural Development*, vol. 22, pp. 1686–1692, 2019.
- [25] K. Johansen, T. Raharjo M. F. McCabe, “Using multi-spectral UAV imagery to extract tree crop structural properties and assess pruning effects” *Remote Sensing*, vol. 10, no. 6, p. 854, 2018.
- [26] L. Liao, L. Cao, Y. Xie, J. Luo and G. Wang, “Phenotypic traits extraction and genetic characteristics assessment of eucalyptus trials based on UAV-borne LiDAR and RGB images,” *Remote Sensing*, vol. 14, no. 3, p. 765, 2022.
- [27] X. Dong, Z. Zhang, R. Yu, Q. Tian and X. Zhu, “Extraction of information about individual trees from high-spatial-resolution UAV-acquired images of an orchard,” *Remote Sensing*, vol. 12, no. 1, p. 133, 2020.
- [28] J. Tian, T. Dai, H. Li, C. Liao, W. Teng, Q. Hu, ... and Y. Xu, “A novel tree height extraction approach for individual trees by combining TLS and UAV image-based point cloud integration,” *Forests*, vol. 10, no. 7, p. 537, 2019.
- [29] S. Abdullah, K. N. Tahar, M. F. A. Rashid and M. A. Osoman, “Estimating tree height based on tree crown from UAV imagery,” *Malaysian Journal of Sustainable Environment*, vol. 9, no. 1, pp. 99–118, 2022.

- [30] X. Wang, Y. Wang, C. Zhou, L. Yin and X. Feng, "Urban-forest monitoring based on multiple features at the single tree scale by UAV," *Urban Forestry & Urban Greening*, vol. 58, p. 126958, 2021.
- [31] G. Vacca E. Vecchi, "UAV photogrammetric surveys for tree height estimation," *Drones*, vol. 8, no. 3, p. 106, 2024.
- [32] M. Oh, E. Jung, H. Lim, W. Song, S. Hu, E. M. Lee, ... and H. Myung, "TRAVEL: Traversable ground and above-ground object segmentation using graph representation of 3D LiDAR scans," *IEEE Robotics and Automation Letters*, vol. 7, no. 3, pp. 7255-7262, 2022.
- [33] M. J. Heaton, A. Datta, A. O. Finley, R. Furrer, J. Guinness, R. Guhaniyogi, ... and A. Zammit-Mangion, "A case study competition among methods for analyzing large spatial data," *Journal of Agricultural, Biological and Environmental Statistics*, vol. 24, pp. 398-425, 2019.
- [34] J. Braun, H. Braunova, T. Suk, O. Michal, P. Petovsky and I. Kuric, "Structural and geometrical vegetation filtering-case study on mining area point cloud acquired by UAV Lidar," *Acta Montanistica Slovaca*, vol. 26, no. 4, 2021.
- [35] E. Mavridou, E. Vrochidou, G. A. Papakostas, T. Pachidis and V. G. Kaburlasos, "Machine vision systems in precision agriculture for crop farming," *Journal of Imaging*, vol. 5, no. 12, p. 89, 2019.
- [36] S. A. Bhat, O. Bashir, S. A. U. Haq, T. Amin, A. Rafiq, M. Ali, ... and F. Sher, "Phytoremediation of heavy metals in soil and water: an eco-friendly, sustainable and multidisciplinary approach," *Chemosphere*, vol. 303, p. 134788, 2022.
- [37] J. Iglhaut, C. Cabo, S. Puliti, L. Piermattei, J. O'Connor and J. Rosette, "Structure from motion photogrammetry in forestry: a review" *Current Forestry Reports*, vol. 5, pp. 155-168, 2019.
- [38] M. Mohan, C. A. Silva, C. Klauberg, P. Jat, G. Catts, A. Cardil, ... and M. Dia, "Individual tree detection from unmanned aerial vehicle (UAV) derived canopy height model in an open canopy mixed conifer forest," *Forests*, vol. 8, no. 9, p. 340, 2017.
- [39] S. Kameyama and K. Sugiura, "Estimating tree height and volume using unmanned aerial vehicle photography and SfM technology, with verification of result accuracy," *Drones*, vol. 4, no. 2, p. 19, 2020.
- [40] D. B. Paz, K. Henderson and M. Loreau, "Agricultural land use and the sustainability of social-ecological systems," *Ecological Modelling*, vol. 437, p. 109312, 2020.
- [41] N. C. Swayze, W. T. Tinkham, J. C. Vogeler and A. T. Hudak, "Influence of flight parameters on UAS-based monitoring of tree height, diameter, and density," *Remote Sensing of Environment*, vol. 263, p. 112540, 2021.